



ELSEVIER

International Journal of Mass Spectrometry 188 (1999) 87–93



# In situ optimization of the electrode geometry of the quadrupole ion trap

Lynn A. Gill, Jonathan W. Amy, Weldon E. Vaughn, R. Graham Cooks\*

Department of Chemistry, Purdue University, West Lafayette, IN 47907, USA

Received 10 June 1998; accepted 24 September 1998

## Abstract

The performance of the quadrupole ion trap is affected by imperfections in the quadrupolar electric fields used to trap the ions. These effects can be compensated for by stretching the trap along its axis. A systematic investigation of the effects of stretching and compressing the  $z_0$  dimension of the ion trap under operating conditions shows improvement in resolution and signal intensity if the  $z_0$  dimension of the quadrupole ion trap is stretched by 9%, with respect to the value for the nominally pure quadrupolar trap. A plot of the relationship between the mass shift for the nitrobenzene molecular ion and  $z_0$  is also presented. It shows that the shift drops to zero at the geometry at which the performance is optimized. (Int J Mass Spectrom 188 (1999) 87–93) © 1999 Elsevier Science B.V.

*Keywords:* Quadrupole ion traps; Electrode geometry; In situ optimization; Mass spectrometry

## 1. Introduction

The quadrupole ion trap can be interfaced to various external ionization sources, can yield signals for ions of mass-to-charge ranges of up to 70 000 Th [1], is capable of providing a resolution greater than  $10^6$  [2–4], and can be used to carry out up to 12 sequential stages of mass analysis [5]. Commercial instruments are available with mass-to-charge ranges of up to 4000 Th with unit mass resolution and up to 10 stages of MS<sup>n</sup> can be performed. In spite of these attributes there is still a desire to improve the performance of this instrument, especially in terms of mass measurement accuracy. In a mathematically pure

quadrupole ion trap the radio frequency (rf) trapping field increases linearly in both the  $z$  and  $r$  directions. However, in actual devices field nonlinearities are present which include hexapole and octapole components. To optimize the performance of the ion trap mass spectrometer, more information is needed on the optimum geometry of the trap; for this reason, a systematic study of the  $r_0/z_0$  ratio as it affects performance was undertaken.

The theoretical or “ideal” spacing between the trap center and the end-cap electrodes in a system that incorporates a 1 cm internal radius ring electrode is 0.707 cm (i.e.  $r_0^2 = 2z_0^2$ , although other choices are also possible if the electrodes’ shapes are modified [6]). This geometry yields a pure quadrupolar field provided electrode truncation, apertures and distortions are ignored. However, the first commercial traps did not employ this geometry but instead used a value

\* Corresponding author. E-mail: cooks@purdue.edu

Dedicated, in admiration, to Brian Green, an instrumentalist *par excellence*.

of  $z_0 = 0.783$  cm [7,8]. This is equivalent to a 10.7% stretch of the end-cap spacing along the  $z_0$  axis. This value was used to eliminate mass shifts observed for some compounds that were ascribed to contributions of higher order fields. Truncation of electrodes, machining imperfections, assembly tolerances and apertures in the electrodes all have been shown to cause the trapping field to deviate from the pure quadrupolar field [9,10]. The nonlinearities found in a quadrupole ion trap can be described by a weighted sum of the superposition of higher-order multipole fields, the hexapole and octapole terms being especially important [11]. It is important to note that the higher-order multipole fields slightly change the motion of the ions and introduce nonlinear resonances and other nonlinear effects [10]. The results of the  $z_0$  stretch are to introduce a positive octapolar field component that offsets the contributions with negative coefficients that arise from field imperfections. The present approach effectively consists of compensating for unavoidable nonlinearities in the field by intentionally introducing other offsetting nonlinearities. Gabrielse and Mackintosh faced the same problem and used the same method in trying to improve the performance of the Penning trap [12]. Note that an alternative approach is to attempt to compensate for the higher-order field components using additional lens elements that can be activated as needed [13]. Yet another approach is to employ an electrode system designed to give a more perfect quadrupolar field, and this has been implemented by a variety of authors in Penning traps [14–17].

In the development of the quadrupole ion trap, as early as 1984 it was recognized that nitrobenzene was incorrectly being assigned to a  $m/z$  of 122 Th (correct mass 123 Th) [8]. Many reasons were initially given, however, all were eliminated except the possibility that field imperfections caused the shift. Syka [8] investigated whether or not changing the trap geometry could change this mass shift and suggested that spreading the end-cap electrodes would eliminate the mass shifts. They found that by increasing the distance between the end-cap electrodes by 0.075 cm from the original ideal geometry ( $z_0 = 0.707$  cm,  $r_0 = 1.0$  cm) the mass shift for nitrobenzene was

eliminated, but if only a 0.051 cm stretch was incorporated a mass shift for nitrobenzene was still observed. These experiments provided a solution to the immediate problem of incorrect nominal mass-to-charge assignments and there the matter rested for some time.

A later study of compound dependent mass shifts by Cleven et al. [18] found an effect related to the field-dependent mass shifts upon increasing the spacing of the end-cap electrodes from that of the ideal geometry. Laser tomography studies showed that the dimension of the ion cloud expands along the radial axis as the number of ions in the trap increases. Furthermore, this increase in width of the distribution correlates with an increase in apparent mass measured. The ion cloud size is compound dependent, and again, stretching the trap reduces this effect.

From these earlier experiments, as well as reports from this lab [1] and by Traldi and co-workers [19–21], it is evident that the geometry of the quadrupole ion trap plays an important role in its performance. However, systematic studies were not reported and the origin of the mass shifts is not yet explained. In order to systematically study effects of the  $r_0/z_0$  ratio on ion trap performance, a system for varying the  $z_0$  dimension under operating conditions was designed and built. Three factors were investigated in assessing the performance of the trap as a function of the  $z_0$  dimension: resolution, intensity and mass shifts relative to fluorocarbon ions.

## 2. Experimental

All experiments used a prototype ion trap mass spectrometer (ITMS) with  $r_0 = 1.0$  cm and  $z_0 = 0.783$  cm before modification. The original instrument is described elsewhere [22] and the modifications to this system are described here. In order to adjust  $z_0$  *in situ* a mechanical system was designed that allowed for the variation of  $z_0$  without the need to vent the system. To implement this feature a linear micrometer (MDC Corp. Hayward, CA) with a metal seal flange was attached to one of the ConFlat flanges on the ITMS vacuum chamber. The linear micrometer

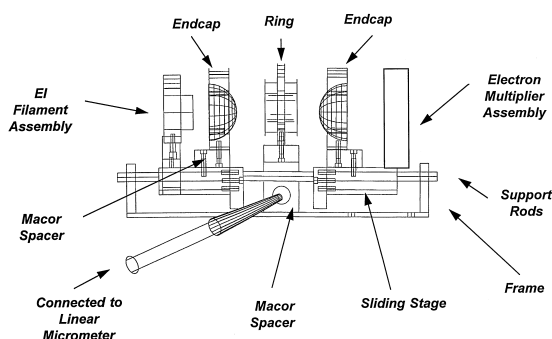


Fig. 1. Experimental setup utilizing a linear micrometer to systematically stretch the quadrupole ion trap along the  $z_0$  axis under operating conditions.

has 2 in. (5 cm) of linear travel delineated by 0.001 in. ( $2.54 \times 10^{-3}$  cm) laser etched travel graduations. As seen in Fig. 1, a tapered rod connected to the linear micrometer systematically spreads the two end-cap electrodes mounted on moving stages. This arrangement allows  $z_0$  to be varied from 0.684 to 0.920 cm which corresponds to the range from  $-3.3\%$  to  $+30.1\%$  of the ideal  $z_0$  value of 0.707 cm. The micrometer allowed for incremental adjustments of the  $z_0$  spacing by  $0.003 \pm 0.001$  in. ( $0.0076 \pm 0.0025$  cm). The spacing between the entrance end-cap and ring electrode and the spacing between the exit end-cap and the ring electrode differed by 0.005 in. (0.01 cm) which is similar in magnitude to the machining tolerance of the electrodes.

It is critical that the motion of the micrometer is purely linear and not rotational to maintain parallel alignment of the end-cap electrodes. The moving stages that support the end-cap electrodes are constructed of stainless steel and each contains four bearings that allow them to slide smoothly along two stainless-steel support rods. This dual-rod system helps maintain the parallel orientation of the end-cap electrodes and prevents binding during  $z_0$  extension. The end-caps are electrically isolated from the stages with ceramic spacers (Macor, Corning Corp. Corning, NY). Macor is also used to isolate the ring electrode from the stainless steel support frame. The electron impact (EI) filament assembly, used for internal EI ionization, and the electron multiplier are mounted on the moving stages to maintain a constant distance to

their respective end caps. This system is housed in the ITMS cradle and is operated using the ITMS electronics. Data are acquired using a digital oscilloscope (Tektronix Model TDS 540) that receives the electron multiplier signal after it has passed through the standard ITMS preamplifier.

Experiments were performed with a single-holed entrance end-cap electrode and a seven-holed exit end-cap electrode. The entrance end-cap electrode has a hole diameter of 0.046 in. (1.2 mm) and the exit end-cap electrode has a hole diameter of 0.052 in. (1.3 mm). The rf coil was tuned at each new  $z_0$  setting to balance the rf circuit. To tune the rf coil, the tuning screw was adjusted until the rf modulator, observed in the instrument software control panel, had a maximum value of 2000 V and an average value of 550 V. Helium was used as the buffer gas at uncorrected pressures of both  $2 \times 10^{-5}$  and  $2 \times 10^{-4}$  Torr. The sample pressure for nitrobenzene was  $4.4 \times 10^{-7}$  Torr (uncorrected) and that for perfluorotributylamine was  $6 \times 10^{-7}$  Torr (uncorrected). Samples were used as received and introduced into the vacuum chamber through separate Granville Philips leak valves.

Standard mass-selective instability scans, without the application of axial modulation or resonance ejection, were used to eject the ions from the trap and so record mass spectra. Mass assignments were made by recording both the time of ejection (measured on the oscilloscope) and the assignment given by the ITMS data system. The more precise value, that from the digital oscilloscope, was plotted and is used in the data presented in this article. Full width at half maximum values (FWHM) and peak intensities were recorded to provide information on the resolution and performance achieved at each new geometry.

### 3. Results and discussion

The hyperbolic trap mounted on a moving stage allows the axial dimension,  $z_0$ , of the ion trap to be compressed and expanded *in situ*. This apparatus provides the opportunity to systematically study the resolution and signal intensity as a function of the geometry of the ion trap. The ability to control the

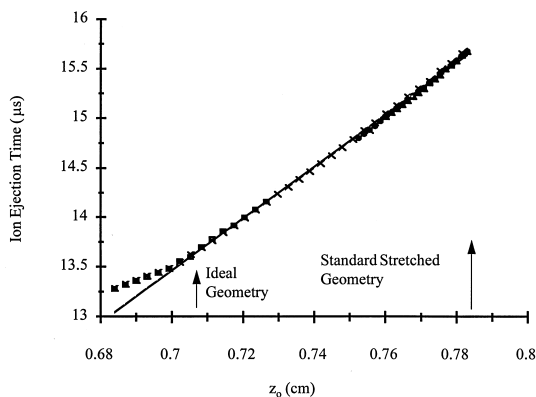


Fig. 2. Reproducibility of ion ejection times for the 123 Th ion of nitrobenzene for various  $z_0$  positions. Ejection time is measured from the start of the rf ramp until the time of detection. The different symbols represent different days of data collection and the line is a linear fit to the data.

geometry of an ion trap mass spectrometer under operating conditions is a new capability.

The relationship between ion ejection time and the value for  $z_0$  is displayed in Fig. 2, which shows data for the molecular ion of nitrobenzene. In this experiment a relatively low helium bath gas pressure of  $6 \times 10^{-6}$  Torr (uncorrected) was used. After internal ionization ( $\sim 5$  ms) the ions were allowed to cool for 20 ms before being ejected from the trap by a rf ramp. These experiments also served to characterize the performance of the moving stage, since experiments were carried out over a 2-week period and the different symbols represent data recorded on different days. The results of a linear fit are also displayed although the following ion trap mass analysis equation [23], leads one to expect curvature as is observed in the plot:

$$\frac{m}{z} = \frac{8V}{q\Omega^2 (r_o^2 + z_o^2)} \quad (1)$$

In Eq. (1)  $m$  is the mass of the ion,  $z$  is the charge,  $V$  is the rf potential required to eject the ions,  $q$  is the  $q_z$  value of ejection,  $\Omega$  is the rf drive frequency, and  $r$  and  $z$  are the trap dimensions. Similar results were found for the 131 Th peak of perfluorotributylamine (PFTBA) (data not shown). The ion ejection times are measured from the start of the rf ramp to the time of

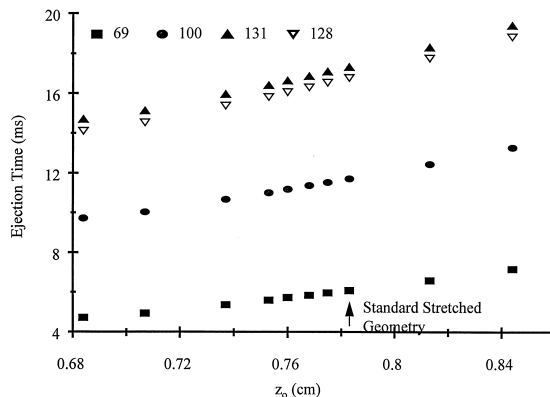


Fig. 3. Ejection times at different  $z_0$  positions for the 69, 100, and 131 Th fragment ions of perfluorotributylamine and the 128 Th molecular ion of  $d_5$ -nitrobenzene.

ion detection for  $z_0$  values that vary from  $-3.3\%$  to  $+30.1\%$  of the ideal  $z_0$  value of 0.707 cm. The reproducibility of this data shows that the  $z_0$  end-cap spacing can be set to  $0.003 \pm 0.001$  in. ( $0.0076 \pm 0.0025$  cm). At low  $z_0$  values, i.e.  $z_0 < 0.7$  cm, the relationship between ejection time and trap  $z$  dimension is nonlinear. This result is not unexpected because at smaller values of  $z_0$  the ions experience increasingly large nonlinear fields.

Fig. 3 shows results for the 69, 100, and 131 Th ions of perfluorotributylamine and the molecular ion of  $d_5$ -nitrobenzene (128 Th). In this experiment the helium bath gas pressure was considerably higher,  $2 \times 10^{-4}$  Torr (uncorrected), and the analyte pressure was maintained at  $4.4 \times 10^{-7}$  Torr (uncorrected). The same ionization time, cooling time and ejection method were used. Again these plots are approximately linear.

To characterize the performance of the trap over the range of  $z_0$  dimensions described previously, the FWHM values and the maximum peak intensities were recorded using the digital oscilloscope for ions of  $m/z$  123 Th generated from nitrobenzene and  $m/z$  131 Th generated from PFTBA. These experiments were first attempted with PFTBA and nitrobenzene in the trap simultaneously, however, it was difficult to regulate the individual analyte pressures. Subsequently, each compound was introduced into the trap separately to allow fluctuations in analyte pressure to

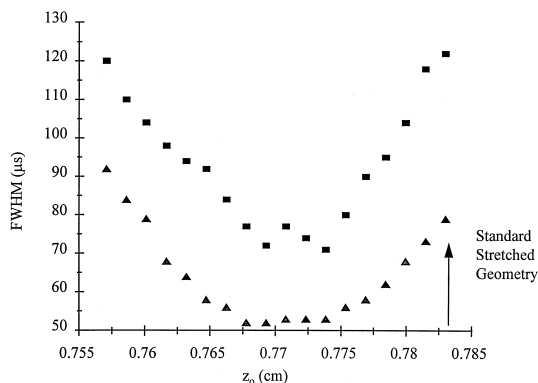


Fig. 4. Plot of FWHM values for the  $^{131}\text{Th}$  ion of perfluorotributylamine (closed triangle), and the  $^{123}\text{Th}$  ion of nitrobenzene (closed square). Each ion species was measured individually. Note that the optimum FWHM value is less than the standard  $z_0$  stretch of 0.783 cm.

be detected and corrected. The lower helium pressure,  $2 \times 10^{-5}$  Torr (uncorrected), was chosen for these experiments. It is interesting to note that the FWHM values are improved for axial dimension  $z_0 < 0.783$  cm (i.e. less than the standard stretched geometry). Looking at the data for nitrobenzene, presented in Fig. 4, the smallest peak width occurs when  $z_0$  is between 0.7675 and 0.775 cm. This corresponds to a 8.5%–9.6% stretch (i.e.  $r_0/z_0 = 1.304 - 1.290$ ) which is significantly different from the standard stretch of 10.7% ( $r_0/z_0 = 1.277$ ). In addition, the FWHM for the  $^{131}\text{Th}$  ion of perfluorotributylamine minimizes at  $z_0$  values similar to those found for the  $^{123}\text{Th}$  ion of nitrobenzene. It is important to note on this plot the performance recorded using the standard stretch of 10.7%, equivalent to  $z_0 = 0.783$  cm. Working at the optimum value provides an improvement in resolution of approximately a factor of two for both perfluorotributylamine and nitrobenzene.

The helium bath gas pressure of  $2 \times 10^{-5}$  Torr (uncorrected) used in these experiments is an order of magnitude less than the standard operating pressure of  $2 \times 10^{-4}$  Torr (uncorrected). Therefore, additional experiments were performed at a helium pressure of  $2 \times 10^{-4}$  Torr (uncorrected) to check what effect the bath gas pressure had on the FWHM values. The results for the  $^{131}\text{Th}$  ion of perfluorotributylamine are presented in Fig. 5. From this plot it can be seen

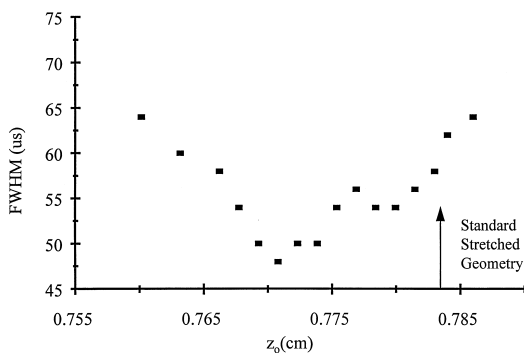


Fig. 5. FWHM values for the  $^{131}\text{Th}$  ion of perfluorotributylamine at a helium bath gas pressure of  $2 \times 10^{-4}$  Torr (uncorrected).

that the improvement in resolution is not as pronounced, however a decrease in the  $z_0$  spacing from the standard stretched geometry ( $z_0 = 0.783$  cm) still leads to improved performance.

Peak intensity is a complementary characteristic that can be used to judge trap performance. These experiments were again carried out at lower and higher helium bath gas pressures. Fig. 6 displays the results for  $^{123}\text{Th}$  molecular ion of nitrobenzene at a helium pressure of  $2 \times 10^{-5}$  Torr (uncorrected). These results correlate well with the FWHM values displayed in Fig. 4 and suggest that the optimum stretch is about 8.7%. At a higher helium bath gas

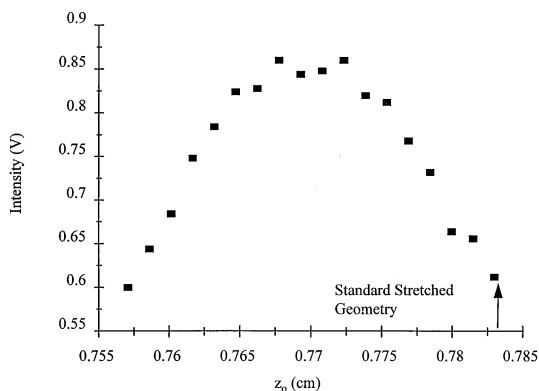


Fig. 6. Plot of maximum signal intensity for the  $^{123}\text{Th}$  molecular ion of nitrobenzene at a helium bath gas pressure was  $2 \times 10^{-5}$  Torr (uncorrected). These data again show an improvement in signal intensity at a stretch less than the standard  $z_0$  dimension of 0.783 cm.

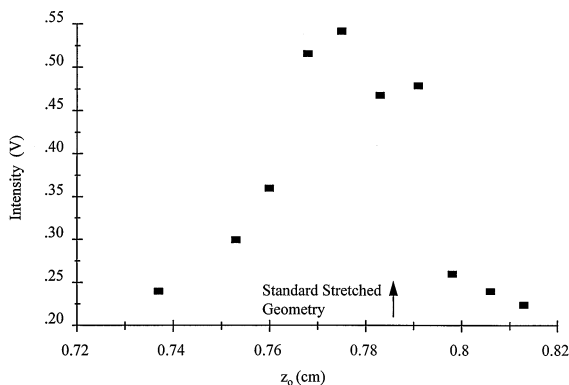


Fig. 7. Plot of the maximum signal intensity of the 69 Th fragment ion of perfluorotributylamine at a helium bath gas pressure of  $2 \times 10^{-4}$  Torr (uncorrected).

pressure of  $2 \times 10^{-4}$  Torr (uncorrected) (Fig. 7) the improvement is again not as great as in the case where a lower helium pressure is used. However, improved performance is achieved by decreasing the spacing between the end-cap electrodes in the commercial trap.

Fig. 8 shows the effect that the  $z_0$  value has on the mass shift for the 123 Th molecular ion of nitrobenzene relative to a scale calibrated using the 69, 100, and 131 Th ions of perfluorotributylamine. These experiments were carried out at a helium pressure of  $2 \times 10^{-4}$  Torr (uncorrected). It is evident from Fig. 8 that as  $z_0$  increases the mass shift for nitrobenzene decreases. However, at approximately 0.770 cm this

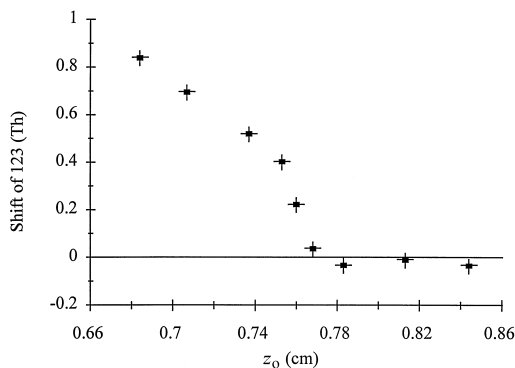


Fig. 8. The effect that changing the end-cap spacing along the  $z_0$  axis has on the mass shift of the molecular ion of nitrobenzene (123 Th).

shift reaches zero and any further stretching does not alter the mass assignment.

#### 4. Conclusion

The systematic stretching of the  $z_0$  axis in the quadrupole ion trap shows that the optimum stretch is less than the standard stretch of 10.7% with respect to the ideal geometry but is still substantial ( $\sim 9\%$ ). Signal intensity and resolution at the optimum stretch were improved and mass accuracy was maintained. The improved performance was determined by measuring the peak FWHM and the maximum peak intensity for nitrobenzene and PFTBA. Both showed improved performance at a  $z_0 = 0.770$  cm (8.9% stretch from the ideal geometry) compared to a pure quadrupole trap where  $z_0 = 0.707$  cm and compared to the standard stretched trap where  $z_0 = 0.783$  cm. The reasons underlying the mass shift have been explored by several groups [8,17,24–27]. Presumably the optimized performance recorded here is simply because the *in situ* adjustment capability allows the higher order field effects to be more accurately compensated for than in the pioneering investigations of Syka [8]. One complication in the experiments was maintaining the partial pressure of two compounds with only one ionization gauge. To improve the quality of the measurements, compounds were measured individually as well as in mixtures.

The mechanical system that was designed and built in this study allows for fine control of the  $z_0$  stretch under operating conditions and could be used in the future to optimize other quadrupole ion traps where modifications to the geometry have been made. For example, in the nondestructive detection experiment [28] the end-caps are modified to accommodate pin electrodes. Field distortions due to these modifications could be minimized by using methods analogous to those presented in the present study.

Improvements in resolution and peak height are associated with geometry optimization. The underlying reasons for the enhanced performance are the subjects of an ongoing investigation.



## Acknowledgements

This project was supported by the Division of Chemical Sciences, Office of Basic Energy Sciences, Office of Energy Research, U.S. Department of Energy and Finnigan Corporation. The authors thank Weldon Vaughn for construction and calibration of the moving stage, and the reviewers for their careful attention and helpful comments.

## References

- [1] R.E. Kaiser, R.G. Cooks, G.C. Stafford, J.E.P. Syka, P.H. Hemberger, *Int. J. Mass Spectrom. Ion Processes* 106 (1991) 79.
- [2] J.D. Williams, K.A. Cox, R.G. Cooks, R.E. Kaiser, J.C. Schwartz, *J. Am. Soc. Mass Spectrom.* 5 (1991) 327.
- [3] J.C. Schwartz, J.E.P. Syka, I. Jardine, *J. Am. Soc. Mass Spectrom.* 2 (1991) 198.
- [4] F.A. Londry, G.J. Wells, R.E. March, *Rapid Comm. Mass Spectrom.* 7 (1993) 43.
- [5] J.N. Louris, J.S. Brodbelt-Lustig, R.G. Cooks, G.L. Glish, G.J. VanBerkel, S.A. McLuckey, *Int. J. Mass Spectrom. Ion Processes* 96 (1990) 117.
- [6] R.D. Knight, *Int. J. Mass Spectrom. Ion Phys.* 51 (1983) 127.
- [7] J. Louris, J. Schwartz, G. Stafford, J. Syka, D. Taylor, *American Society for Mass Spectrometry*, Washington, DC, 1992, p. 1003.
- [8] J.E.P. Syka, in *Practical Aspects of Ion Trap Mass Spectrometry*, R.E. March, J.F.J. Todd (Eds.) CRC, Boca Raton, FL, 1995, Vol. 1, p. 169.
- [9] F. Vedel, M. Vedel, *Phys. Rev. A* 41 (1990) 2348.
- [10] Y. Wang, J. Franzen, *Int. J. Mass Spectrom. Ion Processes* 132 (1994) 155.
- [11] J. Franzen, *Int. J. Mass Spectrom. Ion Processes* 125 (1993) 165.
- [12] G. Gabrielse, F.C. Mackintosh, *Int. J. Mass Spectrom. Ion Processes* 57 (1984) 1.
- [13] J. Franzen, Y. Wang, U.S. Patent No. 5,468,958, 21 November 1995.
- [14] G. Gabrielse, L. Haarsma, S.L. Rolston, *Int. J. Mass Spectrom. Ion Processes* 88 (1989) 319.
- [15] C.D. Hanson, M.E. Castro, E.L. Kerley, D.H. Russell, *Anal. Chem.* 62 (1990) 520.
- [16] P.B. Grosshans, R. Chen, P.A. Limbach, A.G. Marshall, *Int. J. Mass Spectrom. Ion Processes* 139 (1994) 169.
- [17] M. Knobel, K. Wanczek, *Int. J. Mass Spectrom. Ion Processes* 125 (1993) 127.
- [18] C.D. Cleven, R.G. Cooks, A.W. Garrett, N.S. Nogar, P.H. Hemberger, *J. Phys. Chem.* 100 (1996) 40.
- [19] O. Bortolini, S. Catinella, P. Traldi, *Org. Mass Spectrom.* 27 (1992) 927.
- [20] O. Bortolini, G. Spalluto, P. Traldi, *Org. Mass Spectrom.* 29 (1994) 269.
- [21] P. Traldi, D. Favretto, S. Catinella, O. Bortolini, *Org. Mass Spectrom.* 28 (1993) 745.
- [22] J.N. Louris, R.G. Cooks, J.E.P. Syka, P.E. Kelley, G.C. Stafford, J.F.J. Todd, *Anal. Chem.* 59 (1987) 1677.
- [23] R.E. March, R.J. Hughes, *Quadrupole Storage Mass Spectrometry*, Wiley, New York, 1989.
- [24] R.K. Julian, H.P. Reiser, R.G. Cooks, *Int. J. Mass Spectrom. Ion Processes* 123 (1993) 85.
- [25] C.D. Cleven, K.A. Cox, R.G. Cooks, M.E. Bier, *Rapid Commun. Mass Spectrom.* 8 (1994) 451.
- [26] F.A. Londry, R.E. March, *Int. J. Mass Spectrom. Ion Processes* 144 (1995) 87.
- [27] K.A. Cox, C.D. Cleven, R.G. Cooks, *Int. J. Mass Spectrom. Ion Processes* 144 (1995) 47.
- [28] M. Soni, V. Frankevich, M. Nappi, R.E. Santini, J.W. Amy, R.G. Cooks, *Anal. Chem.* 68 (1996) 3314.